Lab on a Chip

Electronic Supplementary Information for

A centrifugal-driven spiral microchannel microfiltration chip for emulsion and deformable particle sorting.

Yongchao Cai, Zekun Li, Cuimin Sun, Xuan Zhao, Shixiong Wu, Guangyong Huang, Shengchang Tang, Peng Dai, Xiangfu Wei, and Hui You

The PDF file includes:

- **Fig. S1.** A detailed description of the process of sample entry and exit in the continuous flow system.
- **Fig. S2.** The serpentine channel in the centrifugal field facilitates the pre-alignment of microdroplets passing through the sorting orifice.
- **Section S1.** Calculation of the droplets' bond number.
- **Movie S1. (.mp4)** The video shows non-homogenous phase emulsion separation experiments.
- **Movie S2. (.mp4)** The video shows homogenous phase emulsion separation experiments.
- **Movie S3. (.mp4)** The video shows arrayed three-component separation experiments.

Supplementary Materials

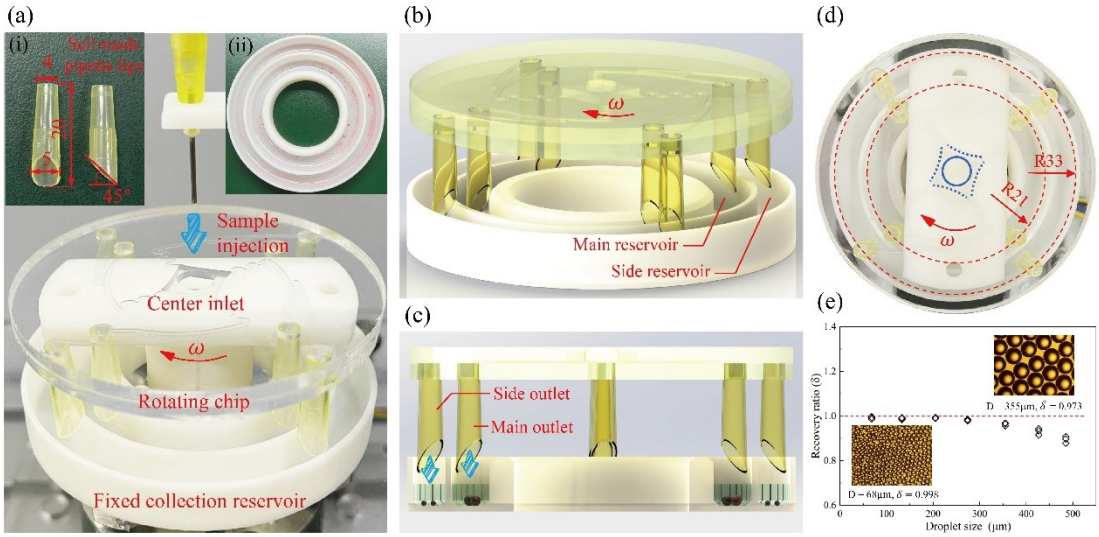

Fig. S1. A detailed description of the process of sample entry and exit in the continuous flow system. (a) The sample was injected into the central inlet of the rotating chip through an injection pump and a conduit. The structure of the inlet, as illustrated by the blue lines in figure (d), consisted of a circular hole with a diameter of 8 mm and an inward concave square groove with a side length of 10 mm. The vertex of the groove was connected to the channel entrance. The difference in diameter between the hole and the groove prevented solution overflow under the centrifugal force. Simultaneously, the inward concave groove guided the solution into the channel under centrifugal force, avoiding any residue within the groove. Since the inlet was located at the center of rotation, sample injection could be achieved during the chip's rotation. It should be noted that before each injection, the channels and inlet groove within the chip need to be pre-filled with a continuous phase (in this case, mineral oil) to eliminate the unpredictable effects of the initial flow of the liquid through the sorting port. **(b)** , **(c)** Schematic and cross-sectional diagrams of the sorting chip and the bottom collection reservoir are shown. Each set of channels had two outlets (main outlet and side outlet), which were connected to self-made pipette tips (as shown in figure (i)). These conduits were fabricated using 200 μL pipette tips with a top diameter of 4 mm for snug connection to the chip outlets and a bottom diameter of 5 mm. They were machined to have a slanted 45° opening to reduce solution residue. The bottom end of the pipette tips was inserted into the main and side collection reservoirs by 3 mm, with the tip facing outward (approximately 1 mm away from the groove sidewall). The collection reservoirs had a width of 7 mm, and a 1 mm chamfer was placed at the bottom corner. Prior to use, the collection reservoirs were pre-filled with a continuous phase, ensuring that the liquid level was maintained between 1-3 mm from the pipette tips, thereby mitigating the impact of the sample. Figure (ii) illustrates the collection reservoir after the droplets have been

collected. **(d)** The main and side outlets of the chip were positioned on concentric circles with radii of 21 mm and 33 mm, respectively, corresponding to the dimensions of the two collection grooves. This arrangement ensured that the pipette tips remained within the collection reservoirs throughout the rotation, enabling the collection of solution during rotation. **(e)** The key to dynamic collection during the rotation process lies in whether the collection process causes any deformation (fragmentation or aggregation) of the droplets. We conducted experiments using a simplified chip without sorting ports, where seven groups of uniform emulsions (particle sizes ranging from 68 to 475 μm) were flown into the side collection reservoir via pipette tips at a maximum speed of 150 rpm. Each experiment was repeated three times, and subsequently, micro-droplets from the collection reservoir were sampled and subjected to random window-based particle size analysis using a metallographic microscope (53X-V, CSOIF, China). The results of the normalized droplet population for the initial particle size are shown in figure (e). The recovery ratio for micro-droplets below 300 μm was above 0.985, and the recovery ratio gradually decreased as the droplet size increased. The majority of droplets in this experiment had sizes smaller than 300 μm, demonstrating that the collection process did not significantly affect the droplet morphology.

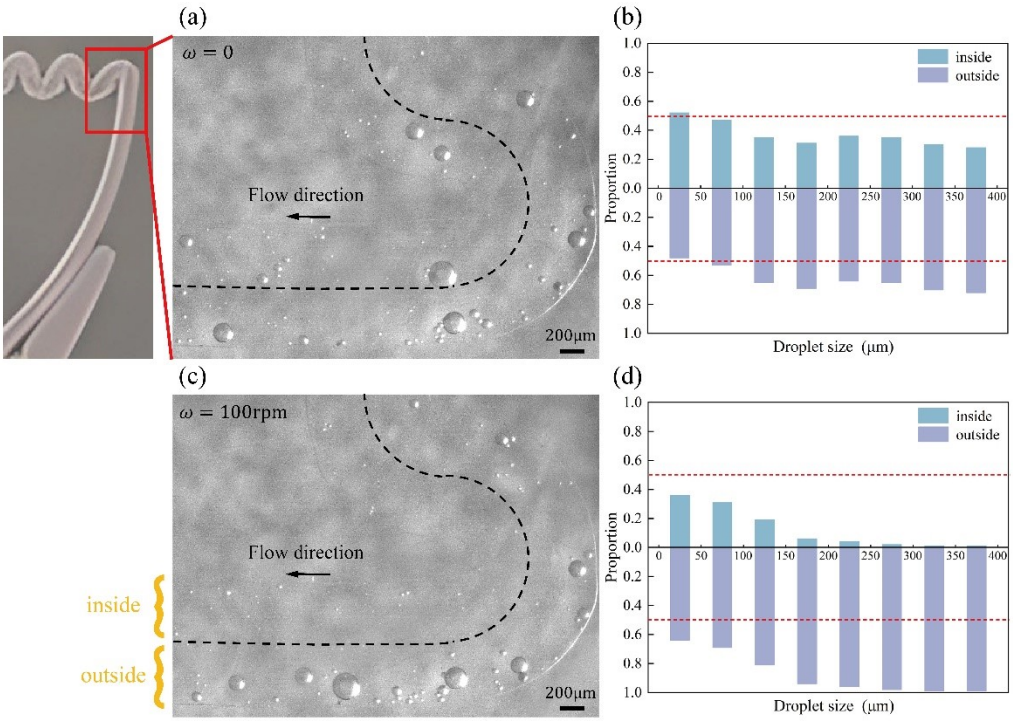

Fig. S2. The serpentine channel in the centrifugal field facilitates the pre-alignment of microdroplets passing through the sorting orifice. (a) The phase diagram of non-homogenous phase emulsion flow through a serpentine channel under capillary action in a stationary state. The black dashed line represents the channel's axis, dividing it into upper and lower sides. In the experiment, the fluid Reynolds number within the microchannel satisfies $Re_f \sim$ (0.015, 0.135) and remains in a laminar flow regime. **(b)** The flow was repeated more than ten times based on the diagram in (a), and the average distribution of microdroplets on both sides of the channel was statistically obtained. The red dashed line represents the 0.5 ratio boundary. The results indicate that the convergence effect of the serpentine channel on microdroplets becomes more pronounced with increasing droplet size, reaching approximately 60% for microdroplets larger than 100 μm. This is attributed to the difficulty of achieving a steady state for the secondary flow within the serpentine channel with alternating curvatures after a few turns (in this case, five turns). Consequently, droplets are primarily influenced by the last curved section of the channel, where the combined effect of inertial lift and Dean drag forces exerted on the droplets directs them towards the outer region of the channel, resulting in a certain degree of convergence. **(c)** and **(d)** depict the phase diagram and droplet size distribution statistics, respectively, of non-homogenous phase emulsion flowing through a serpentine channel under centrifugal force at ω = 100 rpm. Where, the chip rotation direction is clockwise. At this rotational speed, microdroplets exhibit noticeable convergence on the outside of the serpentine channel's outlet. The convergence efficiency for droplets larger than 100 μm reaches above 95%. This is attributed to the increased centrifugal field, which further

influences the microdroplets through the Coriolis force, intensifying their convergence on the outside. Additionally, larger droplets experience stronger inertial Coriolis forces, resulting in higher convergence efficiency. Furthermore, the serpentine channel extends the channel length within a limited radial range, thereby prolonging the duration of inertial forces and also enhancing the convergence effect.

Section S1. Calculation of the droplets' bond number. During the process of microdroplets moving from the inlet to passing through the sorting port, they experience the centrifugal field of the rotating chip. By calculating the droplets' Bond number, we can elucidate the impact of the artificial gravitational field relative to the surface tension of the droplets. The expression for the Bond number is as follows: $$Bo = \frac{F_B}{F_S} = \frac{f_B}{f_S} = \frac{\Delta\rho a L^2}{\sigma}$$, where $\Delta\rho$ is the density difference between the two phases, σ is the interfacial tension, and L is the feature length (i.e. the droplet radius). a is the acceleration associated with the volume force, and in a centrifugal field, $a = \omega^2 r$ is the centrifugal acceleration. In the experiment, the maximum radial value before the droplets reach the sorting port is denoted as r=17.8 mm. The chip rotation speed ranges from 50 to 150 rpm, resulting in an acceleration range of a ~ (0.49–4.39 m/s^2). The droplet sizes range from 60 to 400 μm, with a density difference of $\Delta\rho = \rho_d - \rho_f =$ 176.6 kg/m^3. The interfacial tension between the two phases is taken as σ = 40 mN/m (ASTM). Calculations yield a Bond number range of Bo ~ $(0.0078 - 3.1) \times 10^{-3}$, which is significantly smaller than 1. This indicates that the centrifugal force in the centrifugal field has a negligible influence relative to the surface tension of the droplets. Therefore, the droplets can maintain their spherical shape without significant deformation.

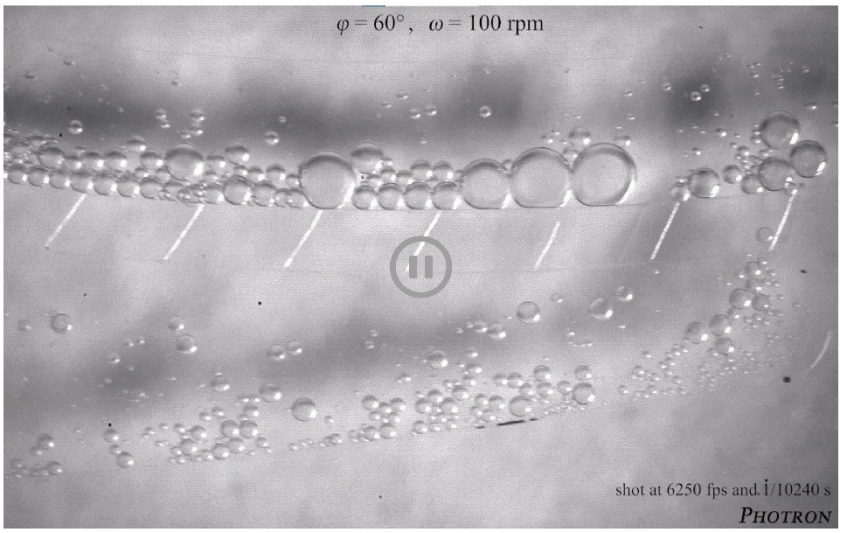

Movie S1. The video shows non-homogenous phase emulsion separation experiments. A non-homogenous phase emulsion with a droplet size range of 0-400 μm was generated using mechanical agitation. Sorting experiments were conducted on chips with three different sorting port angles (φ = 30°, 60°, and 90°) at a fixed rotation speed of ω = 100 rpm (clockwise). The video was recorded at a frame rate of 6250 fps and a shutter speed of 1/10240 s. It was composed by concatenating three sets of video sequences, with each set consisting of 57 frames (equivalent to a duration of 9.12 ms). The presence of a black shadow in the background area of the videos is attributed to the transparent PMMA chip's thickness (similar to a double-sided mirror), which causes the projection of the droplets on the chip's bottom surface.

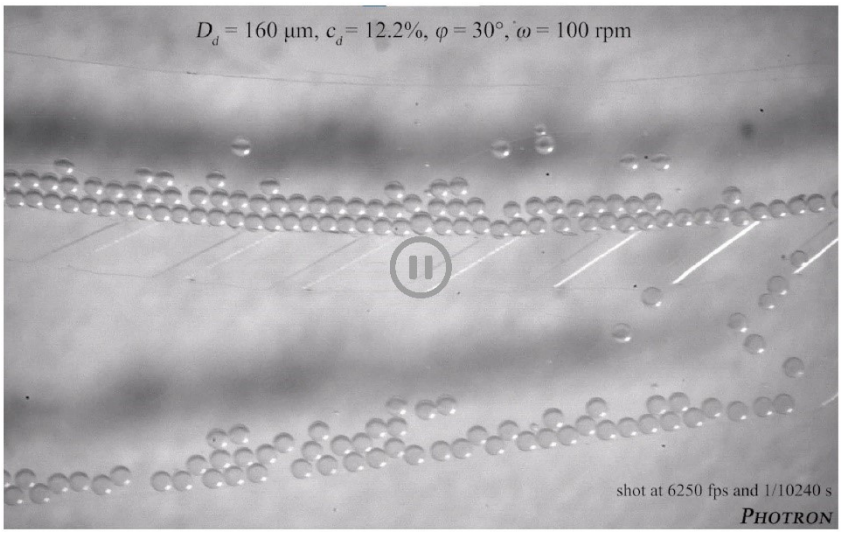

Movie S2. The video shows homogenous phase emulsion separation experiments. In the experiment, homogenous phase emulsions with three different particle sizes, D_d = 60, 160, and 180 μm, were generated using the Co-flow method. Each group of homogenous phase emulsions was diluted to three different concentrations, c_d = 3.8%, 12.2%, and 20.7%, respectively. Subsequently, sorting experiments were conducted on a chip with a sorting port angle of φ = 30° under ω = 100 rpm (clockwise). The video was recorded at a frame rate of 6250 fps and a shutter speed of 1/10240 s. It was composed by concatenating five sets of video sequences, with each set consisting of 60 frames (equivalent to a duration of 9.6 ms). The first three video sequences depict the sorting states of the emulsion with a droplet size of 60 μm at different concentrations. The first, fourth, and fifth video sequences showcase the sorting states of emulsions with different droplet sizes at a concentration of 12.2%. The presence of black shadows in the videos is attributed to the reasons described in Movie S1.

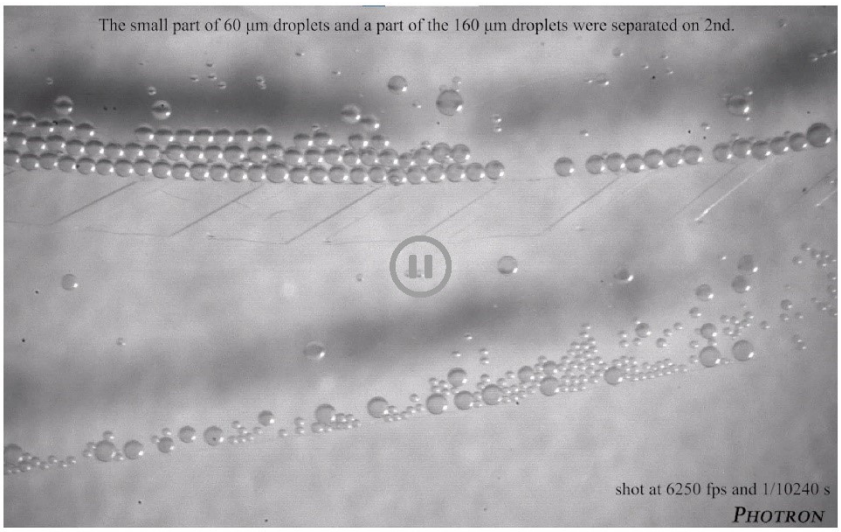

Movie S3. The video shows arrayed three-component separation experiments. Three-component homogeneous-phase emulsions were prepared by combining the homogeneous-phase emulsions (D_d = 60, 160, and 180 μm) with concentrations of c_d = 12.2% in a volumetric ratio of 3:1:1. Sorting experiments were conducted on a chip with φ = 30° and a rotation speed of 100 rpm (clockwise). Due to the unavailability of observation for Chip-II and Chip-III in the arrayed chip, repeated sorting on a single chip was performed as an alternative. The video was recorded at a frame rate of 6250 fps and a shutter speed of 1/10240 s. It was composed by concatenating three repeated sorting videos (referred to as 1st, 2nd, and 3rd), with each set consisting of 60 frames (equivalent to a duration of 9.6 ms). The presence of black shadows in the videos is attributed to the reasons described in Movie S1.